JACS
JOURNAL OF THE AMERICAN CHEMICAL SOCIETY
pubs.acs.org/JACS
Article

Manipulating Attosecond Charge Migration in Molecules by Optical Cavities

Yonghao Gu,* Bing Gu, Shichao Sun, Haiwang Yong, Vladimir Y. Chernyak,* and Shaul Mukamel*

Cite This: J. Am. Chem. Soc. 2023, 145, 14856−14864
Read Online
ACCESS | Metrics & More | Article Recommendations | Supporting Information

ABSTRACT: The ultrafast electronic charge dynamics in molecules upon photoionization while the nuclear motions are frozen is known as charge migration. In a theoretical study of the quantum dynamics of photoionized 5-bromo-1-pentene, we show that the charge migration process can be induced and enhanced by placing the molecule in an optical cavity, and can be monitored by time-resolved photoelectron spectroscopy. The collective nature of the polaritonic charge migration process is investigated. We find that, unlike spectroscopy, molecular charge dynamics in a cavity is local and does not show many-molecule collective effects. The same conclusion applies to cavity polaritonic chemistry.

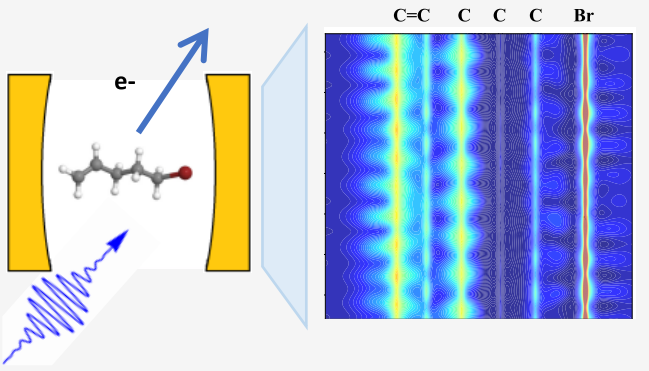

INTRODUCTION

Attosecond laser sources have made it possible to study the coherent electron dynamics of molecular systems in real time.[1,2] Monitoring and manipulating the electronic degrees of freedom in molecules may provide new avenues to control chemical reactions at the early stages of quantum evolution, known as "attochemistry". Upon ionization or photoexcitation of a molecule, ultrafast purely electronic motion before the nuclei have time to move, described by the coherent superposition of multiple electronic states, can now be launched and monitored.[3−9] This process, known as charge migration, was first theoretically predicted by Cederbaum and Zobeley over 20 years ago.[10] Photoinduced charge dynamics is the primary step in many chemical and biochemical reactions,[5] giving rise to possible charge-directed reactivity.[11,12] Developing strategies and techniques for modulating the electronic dynamics is therefore an essential goal of attochemistry.

Optical cavities have proven to be powerful tools for manipulating photophysical and photochemical processes in molecules and materials.[13−19] When the light−matter coupling is stronger than the loss rates of the cavity mode and molecular coherence, vacuum fluctuations of the electric field of the cavity photon mode can couple to the molecular polarization, forming hybrid light−matter states termed polaritons. Molecular electronic (visible) and vibrational (infrared) polaritons have been experimentally and theoretically demonstrated to alter various physical and chemical processes, such as photoisomerization reaction rates, chemical reaction selectivity, optical nonlinearities, and long-range energy transfer.[20−30]

Motivated by the demand for strategies to manipulate coherent electron dynamics, it is interesting to investigate the capability of optical cavities to modify electronic coherence. The ultrafast charge migration process has been theoretically demonstrated as the initial step of charge-directed reactivity is of special interest.[31−34] Despite the numerous theoretical studies of charge migration,[10,31−43] some questions still remain open. One intriguing question is whether there is a systematic way to identify chemical structures that can support charge migration. This issue was recently addressed for halogenated hydrocarbon chains by Lopata et al.[44,45] They find that robust ionization-triggered charge migration processes are supported in conjugated double- and triple-bonded molecules, where the migration modes are $\pi-\pi$ hopping among double or triple carbon−carbon bonds and $p-\pi$ hopping between halogen atoms and carbon π bonds. Saturated unconjugated molecules, in contrast, are predicted to yield a charge hole mostly localized at the halogen atom. In this paper, we investigate the cavity modification of electronic dynamics by enhancing the charge migration in a molecule, where it is otherwise forbidden.

In practice, cavity modification of ultrafast charge migrations and following chemical reactions is carried out by placing many molecules in the cavity. It is important to clarify the collective nature of cavity charge dynamics. For polaritonic spectroscopy, a hallmark of polaritons is that the adsorption spectrum of a

Received: April 12, 2023
Published: June 30, 2023

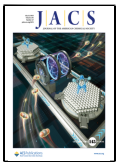

https://doi.org/10.1021/jacs.3c03821
J. Am. Chem. Soc. 2023, 145, 14856−14864

two-level molecule is split into two lines. The resulting Rabi splitting 2κ is collectively enhanced by the number of molecules in the cavity with the effective coupling strength $\kappa = \mu\sqrt{N\hbar\omega_c/2\varepsilon_0 V_c}$, where μ is the transition dipole, ε_0 is the electric permittivity of vacuum, V_c is the cavity mode volume, ω_c is the cavity frequency, and N is the number of molecules. Many previous theoretical studies on cavity-altered photochemistry have been focused on the single and few-molecule strong coupling.[46−50] Most of the experimental demonstrations operate in the collective strong coupling regime, where the coupling strength can be comparable to the cavity frequency $\kappa/\omega_c \approx 0.1-0.2$.[51,52] Despite many recent attempts,[15,53,54] the underlying mechanism under cavity-modified chemistry in the collective regime is not completely understood yet, particularly whether molecules can remain cooperative during a chemical reaction.

In this work, we report a quantum dynamical study of the molecular polariton effects to the charge migration process, whereby an optical cavity mode couples to the coherent superposition of electronic states in photoionized 5-bromo-1-pentene ($BrCH_2CH_2CH_2CH{=}CH_2$) with p (Br) and π (C═C) electron groups separated by carbon single bonds. We find that the long-range charge migration between Br and C═C in the bare molecule upon ionization is very weak due to the absence of a π-conjugated path. The $p-\pi$ hopping mode in this structure is obstructed by the saturated carbon chain. We then analyze the polaritonic charge dynamics with the ionized molecule coupling with an optical cavity mode resonant with the transition between two cation states corresponding to the $p-\pi$ charge holes. We find that in the strong coupling regime, the cavity can significantly enhance the long-range charge migration mode spanning the entire molecule. Our simulations suggest that by forming delocalized hybrid light−matter states, the separated hole distributions at the Br side and C═C sites can couple, leading to a hole-hopping mode between two isolated atomic groups. We predict the signatures of polaritonic charge migration in time-resolved photoelectron spectroscopy (TR-PES), which is sensitive to the attosecond electronic coherence in molecules demonstrated in a theoretical study.[55] To further explore the collective effects in polaritonic charge dynamics, we present a collective ensemble model simulation of many three-level molecules to mimic the many-cation charge migration process. We demonstrate that, unlike the Rabi splitting, charge dynamics of the cations is local and does not show cooperative effects.

THEORY OF QUANTUM DYNAMICS AND TIME-RESOLVED PHOTOELECTRON SPECTROSCOPY

We have simulated the coupling of a single molecule with an optical cavity. The discussion of collective cavity coupling of many cations will be presented in the collective effect study part. We start with a neutral ground state described by Hamiltonian $H_N = \hbar\omega_N|N\rangle\langle N|$. A linearly polarized Gaussian pulse $\boldsymbol{E}(t) = A\vec{\boldsymbol{e}}_0 e^{-i\omega_0 t}e^{-(t^2/2\sigma^2)}$ of peak intensity $I = 1.4 \times 10^{13}$ W/cm^2 (peak amplitude $A = 1.03 \times 10^8$ V/cm), field polarization $\vec{\boldsymbol{e}}_0$, duration $\sigma = 0.3$ fs, and a mean photon energy $\omega_0 = 11.1$ eV is applied to ionize the molecule. This intensity is chosen so that the ground state can be mostly ionized. Some undesired multiphoton processes that could happen are not present in this model. The cation states after ionization are described by Hamiltonian $H_{Cat} = \sum_I \hbar\omega_I|C_I\rangle\langle C_I|$ with I running over the 6 relevant states. Neglecting the Coulomb effect of the cation on the free electron, the free electron Hamiltonian is given by $H_{free} = \sum_{\boldsymbol{k}}\varepsilon_{\boldsymbol{k}}|\boldsymbol{k}\rangle\langle\boldsymbol{k}|$, where $\boldsymbol{k}$ runs over the continuum states of kinetic energy $\varepsilon_{\boldsymbol{k}} = |\boldsymbol{k}|^2/2$. The nuclear motion is assumed to be frozen in the investigated time scale of the electronic motion.

The pulse-driven ionization is calculated by numerically solving the time-dependent Schrödinger equation

$$i\hbar\partial_t|\psi(t)\rangle = (H_0 - \boldsymbol{\mu}\cdot\boldsymbol{E}(t))|\psi(t)\rangle \tag{1}$$

where $H_0 = H_N + H_{Cat} \otimes H_{free}$. The wavefunction $|\psi(t)\rangle$ is a superposition of the neutral ground state $|0\rangle$ and cation-free-electron states $|I\boldsymbol{k}\rangle = |C_I\rangle \otimes |\phi_{\boldsymbol{k}}\rangle$. $\boldsymbol{\mu}$ is the transition dipole moment between $\{|I\boldsymbol{k}\rangle\}$ and $|0\rangle$. The fourth-order Runge−Kutta method is used with a time step of 0.005 fs. The density matrix of cations can then be obtained by tracing the total density matrix over $\boldsymbol{k}$: $\rho(t) = \mathrm{Tr}_{\boldsymbol{k}}\rho^{total}(t)$. In practice, this is described through discretization of $\boldsymbol{k}$ at the angular distributions and the free electron kinetic energies range from 0 to 3.8 eV. The time-dependent electronic charge density of the cation is given by

$$\sigma^{E,Cat}_{total}(\boldsymbol{r}, t) = \sum_I \rho_{II}\sigma^E_{II}(\boldsymbol{r}) + \sum_{I\neq I'} \rho_{II'}(t)\sigma^E_{II'}(\boldsymbol{r}) \tag{2}$$

where $\boldsymbol{r}$ is the spatial coordinate and $\sigma^E_{II}(\boldsymbol{r})$ and $\sigma_{II'}{}^E(\boldsymbol{r})$ are the state charge density and transition charge density, respectively. ρ_{II} is the electronic population, which is time-independent after the pump ionization for; in this study, the nuclei are assumed frozen. $\rho_{II'}(t)$ is the electronic coherence that oscillates with the frequency proportional to the energy difference of the two states I and I'.

The ionization and the photoelectron−cation coupling are generally very fast (within 100 as)[56] compared with the time scale in our study. The coupling of the cavity with the free electron is therefore neglected. The total Hamiltonian of the cation coupled to a single cavity mode can be expressed as

$$H = H_{Cat} + H_{Cav} + H_{CatCav} \tag{3}$$

where the cavity Hamiltonian is $H_{Cav} = \hbar\omega_c(a^\dagger a + 1/2)$ and a and $a^\dagger$ are the cavity-mode annihilation and creation operators, respectively. The cation−cavity interaction is given by the electric-dipole approximation $H_{CatCav} = -\boldsymbol{\mu}\cdot\boldsymbol{E}_c(\boldsymbol{r})$, where

$$\boldsymbol{E}_c(\boldsymbol{r}) = i\sqrt{\hbar\omega_c/2\varepsilon_0 V_c}\, a e^{i\boldsymbol{k}_c\cdot\boldsymbol{r}}\vec{\boldsymbol{e}}_c + \text{H. c.} \tag{4}$$

where $\boldsymbol{k}_c$ is the cavity-mode wave vector, $\vec{\boldsymbol{e}}_c$ is the field polarization, and H.c. stands for the Hermitian conjugate. Cavity coupling strength is defined as $g = \sqrt{\hbar\omega_c/2\varepsilon_0 V_c}$.

The cation polariton states $\{|P_K\rangle\}$ are calculated by diagonalizing the resulting polaritonic Hamiltonian using the direct product basis set $|I, n\rangle = |I\rangle \otimes |n\rangle$, where $\{|n\rangle\}$ are the cavity-photon number states.

The attosecond charge migration can be monitored by TR-PES. This signal, measured as a function of emitted photoelectron kinetic energy ε_k after a probe pulse arriving at time T, was calculated by[55]

https://doi.org/10.1021/jacs.3c03821
J. Am. Chem. Soc. 2023, 145, 14856−14864

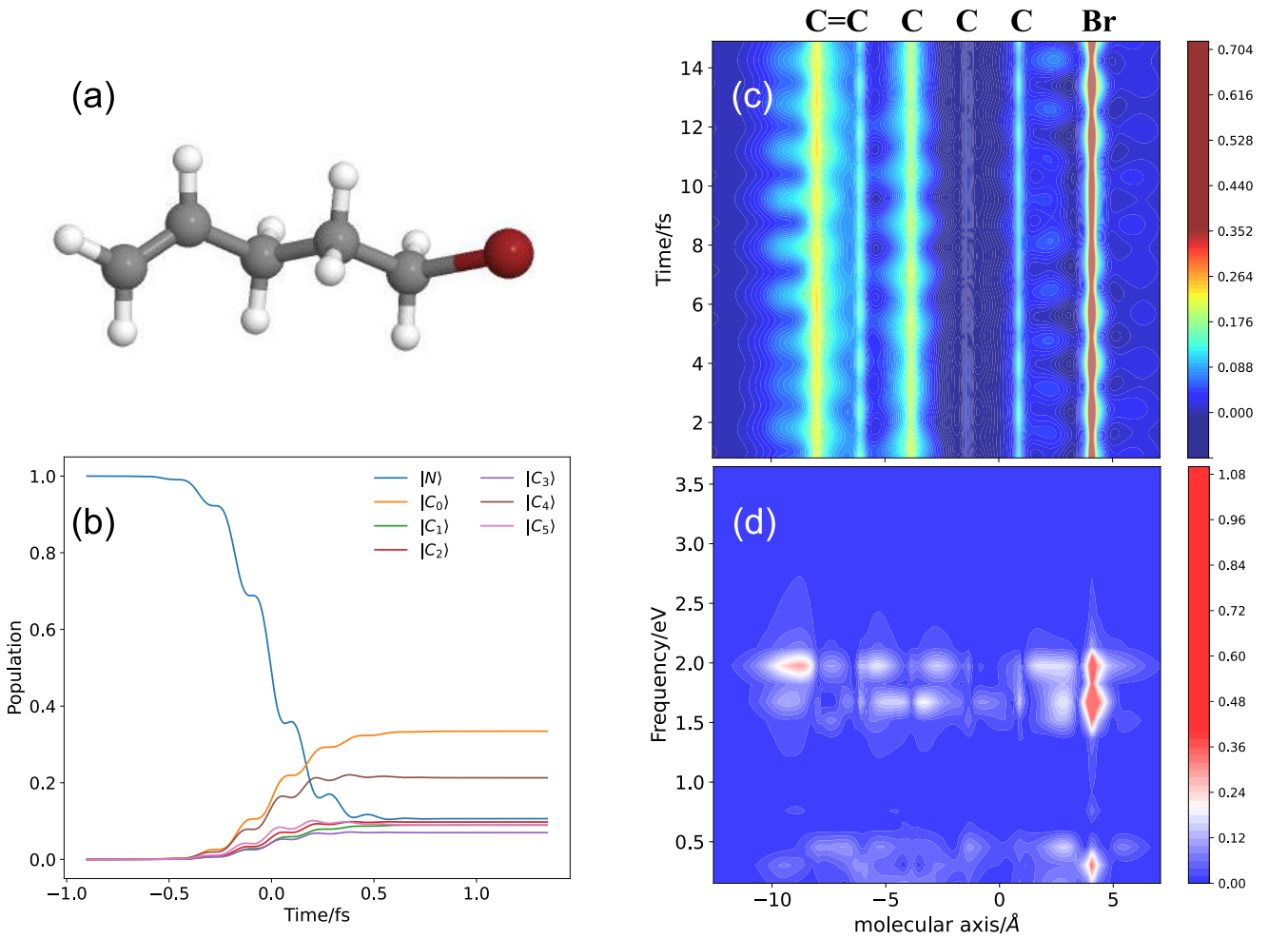

Figure 1. (a) Geometric structure of 5-bromo-1-pentene. (b) Population dynamics of 5-bromo-1-pentene ionized by a pump pulse centered at 11.1 eV. (c) Time-dependent hole charge density of the bare molecule following photoionization. Hole densities are integrated into the molecular axis. (d) Intensity of Fourier transform of the hole charge density in panel (c).

$$S^{\mathrm{TR-PES}}(\varepsilon_{\boldsymbol{k}}, T) = 2\mathcal{R}\mathrm{e}\sqrt{2\varepsilon_{\boldsymbol{k}}} \sum_{KK'} \sum_{\alpha} \int \mathrm{d}\Omega_{\boldsymbol{k}} \rho_{KK'}(t_0) \vec{\boldsymbol{e}}_{\boldsymbol{X}}{}^{*} \cdot V_{K',\alpha\boldsymbol{k}} \vec{\boldsymbol{e}}_{\boldsymbol{X}} \cdot V_{\alpha\boldsymbol{k},K} \cdot \int_{-\infty}^{\infty} \mathrm{d}t \mathcal{E}^{*}(t - T) \mathrm{e}^{-i(\omega_{K'} - \omega_K)(t - t_0)} \int_{0}^{\infty} \mathrm{d}t_1 \mathcal{E}(t - t_1 - T) \cdot \mathrm{e}^{-i(\omega_\alpha + \varepsilon_{\boldsymbol{k}} - \omega_K - \omega_X)t_1} \tag{5}$$

where $\mathcal{E}(t)$ is the XUV probe pulse envelope, $\rho_{KK'}(t_0)$ is the polariton density matrix after the initial ionization, $\vec{\boldsymbol{e}}_{\boldsymbol{X}}$ is the field polarization, $V_{K,\alpha\boldsymbol{k}}$ is the transition dipole moment between $|P_K\rangle$ and $|\alpha\boldsymbol{k}\rangle$, K, K' run over all of the polariton states, and α runs over all of the dication states. The TR-PES signal is given by the sum of the population part ($K = K'$) and the coherence part ($K \neq K'$). At short times where the nuclei are frozen, the population part is time-independent and the coherence part oscillates with the frequencies proportional to the energy differences of the polariton states.

RESULTS AND DISCUSSION

The initialization of charge migration is often modeled by creating a localized charge hole described as a superposition of multiple states, assuming a sudden removal of an electron from a neutral-species orbital.[40,44,57] A recent study shows that such models miss both the phase and the polarization information of the optical field.[41] In this work, we therefore simulate the photoinduced ionization processes explicitly by including the free electron contributions as described before. The population dynamics are shown in Figure 1b. Among the 6 considered cation states, the cation ground state $|C_0\rangle$ and excited state $|C_4\rangle$ are dominant. Their Dyson orbital shapes presented in the Supporting Information reveal that $|C_0\rangle$ is associated with the charge holes of the C=C π bond and Br p orbitals, and $|C_4\rangle$ is associated with the C−H σ bonds of the CH=CH$_2$ group and the C−Br σ bond.

We have first simulated the charge density dynamics of the bare ionized molecule. The motion of the charge hole can be visualized by the time-dependent hole density

$$\sigma^{E,\mathrm{hole}}(\boldsymbol{r}, t) = \sigma^{E,\mathrm{Cat}}_{\mathrm{total}}(\boldsymbol{r}, t) - \sigma^{E,N}_{\mathrm{total}}(\boldsymbol{r}) \tag{6}$$

which is the difference between the time-dependent electronic charge density of the ionized system and the time-independent charge density of the neutral molecule. The time-dependent hole charge density integrated into the molecular axis is shown in Figure 1c. There is no significant charge migration between the C=C side and the Br side upon ionization. The partial charges localized at both ends tend to oscillate only in a very small spatial scale compared to the scale of the whole molecule. This can be illustrated more clearly by the Fourier transform of

https://doi.org/10.1021/jacs.3c03821
J. Am. Chem. Soc. 2023, 145, 14856−14864

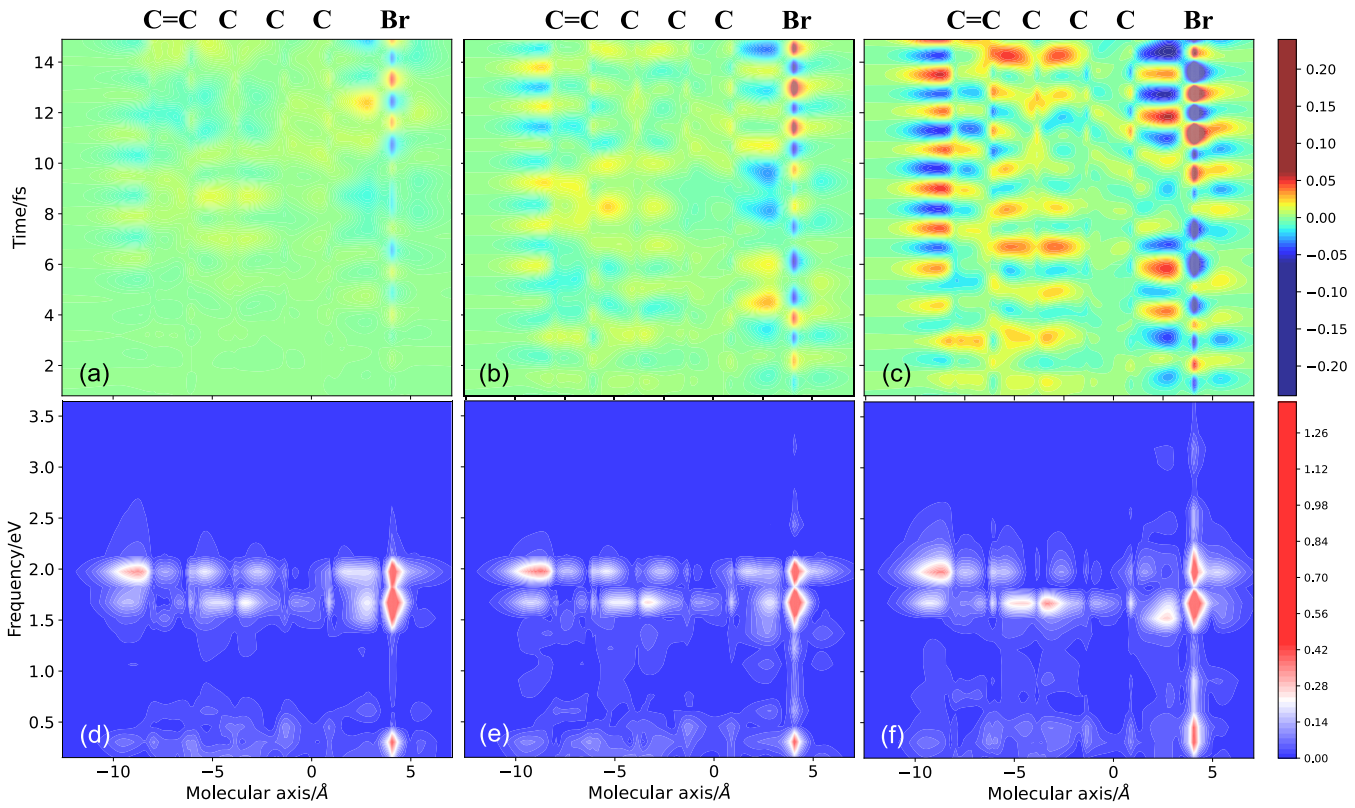

Figure 2. (a–c) Polariton-calculated time-dependent hole density differences (from the bare molecule) for cavity-molecule coupling strengths of 0.0514, 0.154, and 0.257 V/Å, respectively. (d–f) Intensities of Fourier transform of the hole charge densities corresponding to panels (a–c), respectively.

the time-dependent hole density shown in Figure 1d. If two different regions along the molecular axis have comparable intensities at the same frequency, this can be recognized as a charge migration mode between them. At a frequency of ∼2 eV (corresponding to the electronic coherence between $|C_0\rangle$ and $|C_4\rangle$), the intensity of the Br side is much higher than the C═C side, indicating a combination of a weak C═C to Br migration mode with a strong local oscillation mode around the Br atom.

To distinguish the cavity enhanced modes from the oscillation modes in the bare cation, we consider the time-dependent hole density difference as $\Delta\sigma_{\mathrm{cav}}^{E,\mathrm{hole}}(\boldsymbol{r}, t) = \sigma_{\mathrm{cav}}^{E,\mathrm{hole}}(\boldsymbol{r}, t) - \sigma_{\mathrm{bare}}^{E,\mathrm{hole}}(\boldsymbol{r}, t)$. The cavity modification to charge migration mode can thus be visualized as positive–negative patterns oscillating in real time. Figure 2 shows the time-dependent hole density differences calculated for polaritons with cavity frequency ω_c = 1.62 eV and various cavity-molecule coupling strengths. Figure 2a,c shows that the charge migration mode between the C═C side and Br side is gradually enhanced upon increasing the coupling strength. In Figure 2a where the coupling strength is 0.0514 V/Å (0.001 au), the time-dependent hole density differences are negligible, indicating that the influence of the cavity to the charge dynamics is still very weak. However, Figure 2c shows that significant charge migration patterns emerge when the coupling strength increases to 0.257 V/Å. Enhancements of the long-range hopping modes of charge holes can be clearly seen. By analysis of the Fourier transform of time-dependent hole densities in Figure 2d–f, we assign the enhancements into two polaritonic coherence modes at 2 and 1.7 eV, respectively. The former is attributed to the activation of the coherence between $|C_0\rangle$ and $|C_4\rangle$, corresponding to the σ–σ hopping mode between the CH═CH_2 group and the C–Br σ bond. The latter corresponds to the activation of the original $|C_0\rangle$ to $|C_3\rangle$ coherence, representing the p–π migration mode between C═C and Br with the C–C single-bond chain incorporated. Compared to the Fourier transform of bare cation electronic coherence in Figure 1d, the intensities of both the C═C side and C–C single-bond chain in Figure 2f are significantly enhanced, being comparable to the Br side. The activation of long-range charge migration is therefore achieved.

Figure 3 depicts the TR-PES signals of the bare cation and in the cavity with various cavity-molecule coupling strengths. We assume a linearly polarized XUV Gaussian pulse with a mean photon energy of 25 eV and a duration of 0.15 fs as probe light. For the bare cation, the time-independent population part contributions are dominant while the coherence signals are comparatively weak. This agrees with our hole density dynamic simulation results that charge migration is very weak in the bare cation. A robust charge migration mode can only be supported by strong electronic coherence among cation states invoking different localized charge holes. Figure 3c,d shows that the coherence signals are significantly enhanced by the cavity, exhibiting strong time-domain oscillations. As the coupling is increased, additional coherence modes are activated and become clearly resolvable in the time domain. The cavity modification of the electronic dynamics can be effectively monitored by TR-PES compared to the bare cation. In practice, experimental difficulties such as the electron detection of molecules embedded in a cavity must be treated carefully. The detection of ejected electrons at different directions can be influenced by the shape and size of the cavity. High-energy

https://doi.org/10.1021/jacs.3c03821
J. Am. Chem. Soc. 2023, 145, 14856–14864

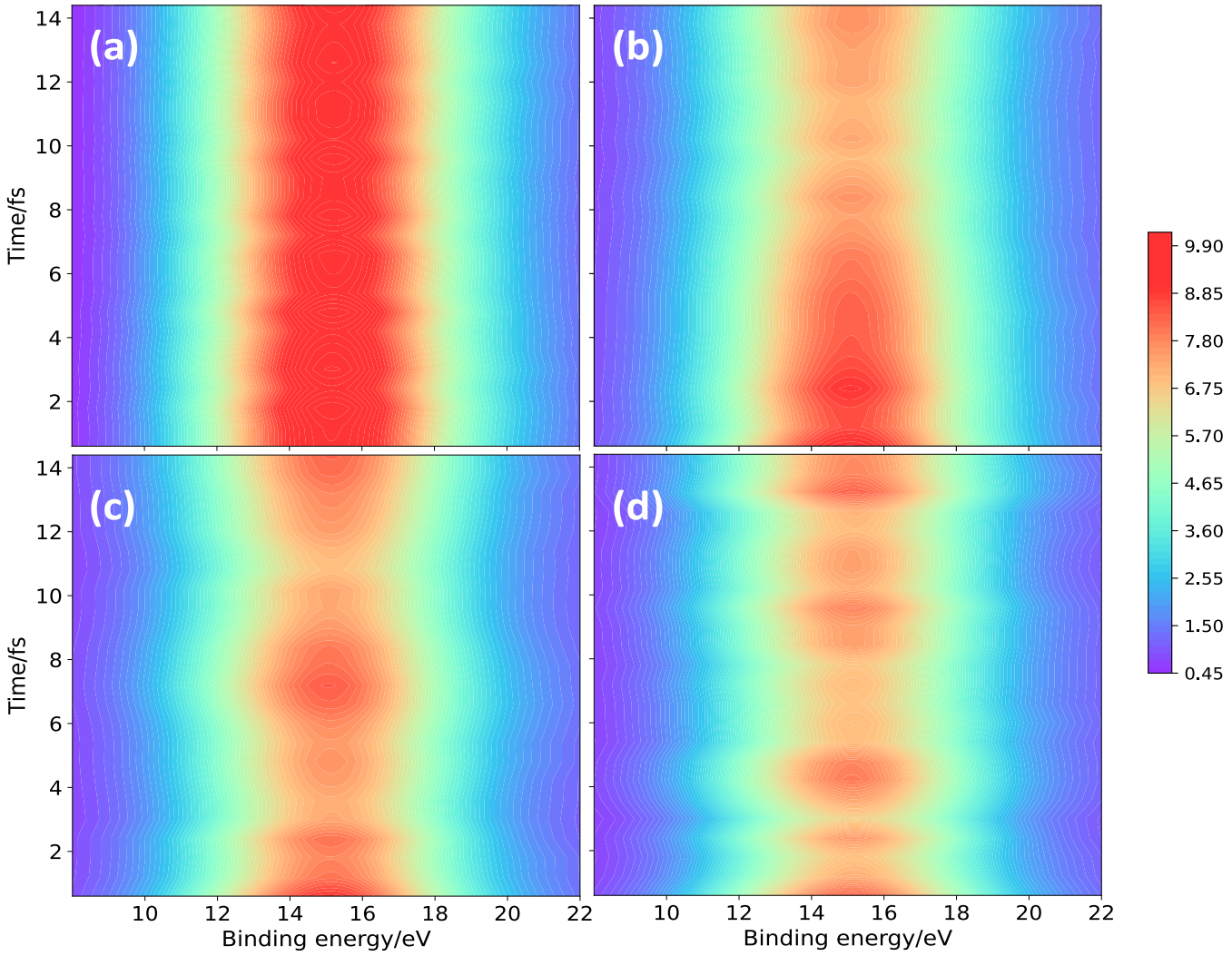

Figure 3. (a) TR-PES signals of the bare cation. (b–d) TR-PES signals of polaritons with cavity-molecule coupling strengths of 0.0514, 0.154, and 0.257 V/Å, respectively. The probe pulse is centered at 25 eV with a duration of 0.15 fs.

resolution cannot be guaranteed in TR-PES with attosecond pulses due to the Fourier uncertainty. To obtain simultaneously high energy and time resolutions, more elaborate techniques such as with entangled light[58] should be employed.

The cavity-detuning variation of time-dependent hole density differences and TR-PES signals of polaritons is presented in Figure 4 for a fixed coupling strength at 0.257 V/Å. From Figure 4a,b, it can be seen that with a positive detuning, two types of migration patterns are significantly activated. These correspond to the patterns between the C and Br atoms at the right side of the molecule and the patterns at the left side of the C=C bond. It is reasonable since when the cavity frequency goes higher, it becomes closer to the energy difference between $|C_0\rangle$ and $|C_4\rangle$. Such a coherence mode with the C−Br σ bond and C−H σ bond in the $CH{=}CH_2$ group is therefore enhanced. On the other hand, as shown in Figure 4c,d, with reducing cavity frequency, its coupling with the $|C_0\rangle - |C_4\rangle$ coherence becomes weaker, resulting in the elimination of the corresponding $\sigma-\sigma$ hopping patterns. The overall detuning results show that robust enhancements can be achieved, regardless of whether the cavity-photon energy is shifted up or down. By setting cavity frequency resonance or off-resonance to specific electronic coherence, it is possible to selectively enhance the desired charge migration mode.

COLLECTIVE EFFECTS IN CAVITY CHARGE DYNAMICS: A MODEL STUDY

The afore-described simulations use a single-molecule cavity model, where local charge dynamics in one cation is studied. We next turn to the collective dynamics of an ensemble of cations. This issue will be addressed through a Tavis–Cummings model (also known as Dicke Model)[59,60] study. The effective coupling strength for an ensemble of N identical molecules with a vacuum cavity mode is usually given by $\kappa = \sqrt{N}g\mu$. The collective effect factor $\sqrt{N}$ is derived from the super-radiance scheme, where the cooperative behavior of indistinguishable molecules is described as the delocalization of molecular dipoles into a giant collective dipole. The corresponding polariton states can be expressed as a superposition of a single excitation shared by all molecules. The $\sqrt{N}$ dependence of Rabi splitting was recently demonstrated by experiments in a rovibrational cavity[61] that it is cooperative. However, molecular charge dynamics invoking only the photoionized states and having no interaction with the unionized neutral ground state cannot

https://doi.org/10.1021/jacs.3c03821
J. Am. Chem. Soc. 2023, 145, 14856–14864

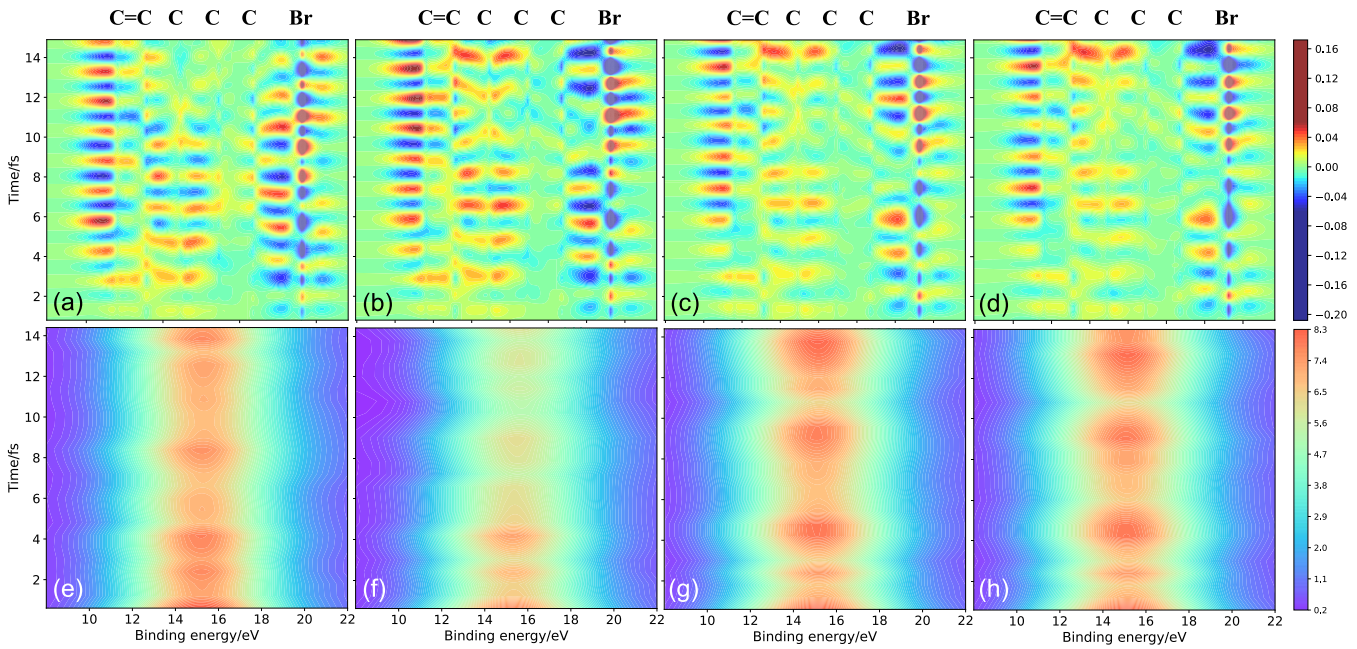

Figure 4. (a–d) Polariton-calculated time-dependent hole density differences (from the bare molecule) for cavity detuning of +0.54, +0.27, −0.14, and −0.27 eV, respectively. The coupling strength is fixed at 0.257 V/Å. (e–h) TR-PES signals correspond to panels (a–d), respectively.

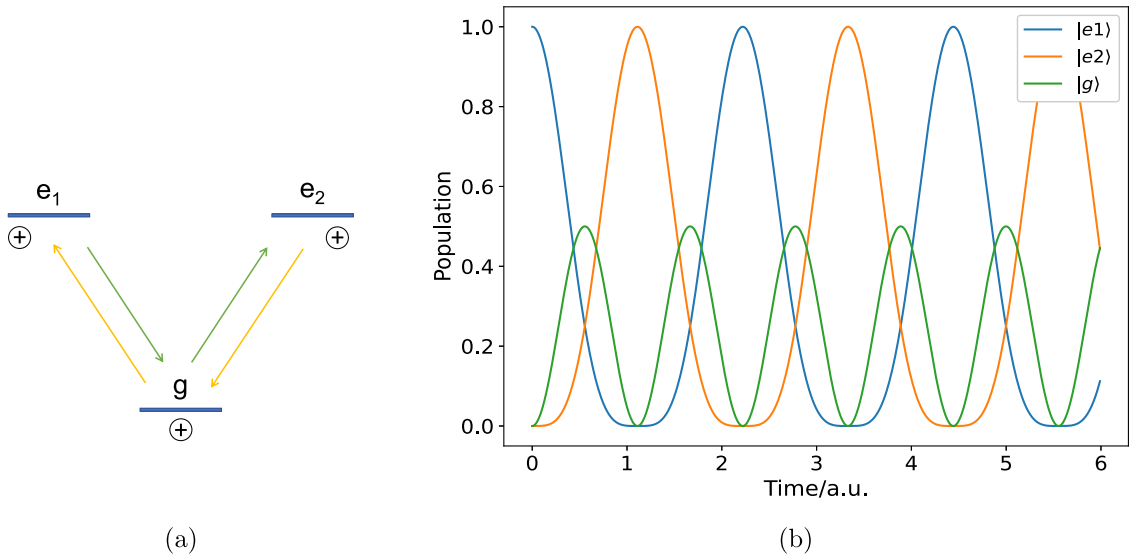

Figure 5. (a) Diagrammatic sketch of the three-level cation system employed in the collective effect study of cavity charge dynamics. (b) Cation state population dynamics calculated from the collective states of N identical three-level cations. Coupling constant g_0 = 1. We numerically calculated for N from 1 to 50 and their population dynamics are virtually the same.

be treated in the same way. A collective ensemble model of cations rather than the delocalized super-radiance model of single excitation should be employed to study the cooperativity in cavity-modified charge migration.

We study a three-level cation system with ground state $|g\rangle$ and two degenerate excited states $|e_1\rangle$ and $|e_2\rangle$, which represent the excited states with the localized charge hole at different sides of a molecule, respectively. The transition between them can thus mimic the charge migration process. We initialize the system of N cations at the $|e_1\rangle$ side. The corresponding collective state is $|e_1^{(1)}e_1^{(2)} \cdots e_1^{(N)},0\rangle$, where $|e_1^{(k)}\rangle$ is the wavefunction of the kth cation and the last number is the cavity-photon number state. In the rotating wave approximation (RWA), the space of excitations includes all of the combinations of k molecules in e_1, l molecules in e_2, and $N - k - l$ molecules in g with $N - k - l$ cavity photons so that the total number of excitations is conserved (N). In the Tavis–Cummings model, we can write all of the combinations in a fully symmetric collective state form

$$|kl\rangle = (C_N^k C_{N-k}^l)^{-1/2} \sum^{C_N^k C_{N-k}^l} |e_1^1 \cdots e_1^k e_2^{k+1} \cdots e_2^{k+l} g^{k+l+1} \cdots g^N, N-k-l\rangle \quad (7)$$

where C_N^k is the combination number of k out of N, and the summation runs over all of the $C_N^k C_{N-k}^l$ combinations of k e_1 and l e_2 out of N cations. For simplicity, we further assume that the transition dipoles $\boldsymbol{\mu}_{g1}$ and $\boldsymbol{\mu}_{g2}$ are symmetric to the cavity-

https://doi.org/10.1021/jacs.3c03821
J. Am. Chem. Soc. 2023, 145, 14856–14864

photon polarization. The nonzero interaction Hamiltonian elements can only take the $H_{kl,k-1l}$ and $H_{kl,kl-1}$ form. These values are given by $H_{kl,k-1l} = \sqrt{k(N-k-l+1)}\,g_0$ and $H_{kl,kl-1} = \sqrt{l(N-k-l+1)}\,g_0$ (see the Supporting Information for detailed derivation). The polariton states are calculated via diagonalization of the total Hamiltonian.

In our three-level cation model, the charge migration process can be directly visualized by the population oscillation between $|e_1\rangle$ and $|e_2\rangle$. The population dynamics of the collective states of N cations (coupling constant $g_0 = 1$) is presented in Figure 5b. We have numerically calculated for the cation number N from 1 to 50 and found that their population behaviors are always the same. The oscillation of migration between $|e_1\rangle$ and $|e_2\rangle$ exhibits no cation number dependence, indicating an absence of cooperativity in molecular charge dynamics. This result is in contrast to the well-known $\sqrt{N}$ dependence of the Rabi splitting, which reflects cooperative super-radiance in the optical response. The interaction Hamiltonian matrix elements in our collective basis contain N-dependent factors of $\sqrt{k(N-k-l+1)}$ and $\sqrt{l(N-k-l+1)}$, and the N-dependency remains in energy splitting of polaritons (corresponding to the cooperativity in spectroscopy). However, those factors cancel out once we calculate a local observable-like charge dynamic in a molecule. The same conclusion can be analytically derived from the two-level system of the Tavis–Cummings model, which has been studied exhaustively in the literature.[62−64]

Note that the initialization of the system can alter the corresponding collective effect. Here, we initialized the system as the most common situation, where local charge holes are created for all of the molecules. In some extreme cases, the conclusions can be different. If the system is initialized with the cation ground state population far more larger than the excited state population, the $\sqrt{N}$ dependency may emerge for charge dynamics.[62] For an ensemble with only one excited cation, the super-radiance model can be restored.

CONCLUSIONS

We have shown how attosecond charge migration in molecules can be manipulated by an optical cavity in the weak to strong cavity-molecule coupling regimes. Application to 5-bromo-1-pentene reveals that a suppressed charge migration modes can be enhanced. In the strong coupling regime, different coherence modes invoking σ-bond hopping and π-bond hopping between unconjugated atomic groups can be activated. Time-resolved photoelectron spectroscopy is predicted to be sensitive to this modulation. To study the local and collective effects in the cavity modification of the charge migration process, we employed a Tavis–Cummings model Hamiltonian of an ensemble of three-level model systems. We showed that super-radiant polariton cooperativity cancels out in the charge dynamics, i.e., increasing the molecule number in the cavity does not affect the charge migration dynamics. It is still possible to achieve pronounced polaritonic effects by decreasing the cavity mode volume. Single-molecule strong coupling has been reported in plasmonic nanocavity experiments.[65] Our results demonstrate that optical cavities can be a powerful means for manipulating the coherent electronic charge dynamics. The present theoretical study was carried out for frozen nuclei. Charge migration creating novel chemistry requires the inclusion of nuclear motions. Extensions of this work by including the nuclear dynamics[40,41,66−68] and exploring topics of charge-directed reactivity are interesting for future studies.

ASSOCIATED CONTENT

Supporting Information

The Supporting Information is available free of charge at https://pubs.acs.org/doi/10.1021/jacs.3c03821.

Results of electronic structure calculation and deviations of the collective model for molecular charge dynamics (PDF)

AUTHOR INFORMATION

Corresponding Authors

Yonghao Gu − *Department of Chemistry and Department of Physics and Astronomy, University of California, Irvine, Irvine, California 92697-2025, United States;* orcid.org/0000-0002-0868-6620; Email: yonghaog@uci.edu

Vladimir Y. Chernyak − *Department of Chemistry, Wayne State University, Detroit, Michigan 48202, United States; Department of Mathematics, Wayne State University, Detroit, Michigan 48202, United States*; Email: chernyak@chem.wayne.edu

Shaul Mukamel − *Department of Chemistry and Department of Physics and Astronomy, University of California, Irvine, Irvine, California 92697-2025, United States;* orcid.org/0000-0002-6015-3135; Email: smukamel@uci.edu

Authors

Bing Gu − *Department of Chemistry, Westlake University, Hangzhou 310030 Zhejiang, China;* orcid.org/0000-0002-5787-3334

Shichao Sun − *Department of Chemistry and Department of Physics and Astronomy, University of California, Irvine, Irvine, California 92697-2025, United States;* orcid.org/0000-0002-7680-3972

Haiwang Yong − *Department of Chemistry and Department of Physics and Astronomy, University of California, Irvine, Irvine, California 92697-2025, United States;* orcid.org/0000-0002-5860-4259

Complete contact information is available at: https://pubs.acs.org/10.1021/jacs.3c03821

Notes

The authors declare no competing financial interest.

ACKNOWLEDGMENTS

This work was primarily supported by the US Department of Energy, Office of Science, Basic Energy Sciences Awards DESC0022134 and DE-FG02-04ER15571 (V.Y.C. and S.M.). B.G. and Y.G. gratefully acknowledge the support of the National Science Foundation through Grant No. CHE-2246379.

REFERENCES

(1) Hentschel, M.; Kienberger, R.; Spielmann, C.; Reider, G. A.; Milosevic, N.; Brabec, T.; Corkum, P.; Heinzmann, U.; Drescher, M.; Krausz, F. Attosecond metrology. *Nature* **2001**, *414*, 509−513.

(2) Paul, P.-M.; Toma, E. S.; Breger, P.; Mullot, G.; Augé, F.; Balcou, P.; Muller, H. G.; Agostini, P. Observation of a train of attosecond pulses from high harmonic generation. *Science* **2001**, *292*, 1689−1692.

(3) Kling, M. F.; Vrakking, M. J. Attosecond Electron Dynamics. *Annu. Rev. Phys. Chem.* **2008**, *59*, 463−492.

(4) Nisoli, M.; Decleva, P.; Calegari, F.; Palacios, A.; Martín, F. Attosecond Electron Dynamics in Molecules. *Chem. Rev.* **2017**, *117*, 10760−10825.
(5) Wörner, H. J.; Arrell, C. A.; Banerji, N.; et al. Charge migration and charge transfer in molecular systems. *Struct. Dyn.* **2017**, *4*, No. 061508.
(6) Goulielmakis, E.; Loh, Z.-H.; Wirth, A.; Santra, R.; Rohringer, N.; Yakovlev, V. S.; Zherebtsov, S.; Pfeifer, T.; Azzeer, A. M.; Kling, M. F.; et al. Real-time observation of valence electron motion. *Nature* **2010**, *466*, 739−743.
(7) Leone, S. R.; McCurdy, C. W.; Burgdörfer, J.; Cederbaum, L. S.; Chang, Z.; Dudovich, N.; Feist, J.; Greene, C. H.; Ivanov, M.; Kienberger, R.; et al. What will it take to observe processes in 'real time'? *Nat. Photonics* **2014**, *8*, 162−166.
(8) Calegari, F.; Ayuso, D.; Trabattoni, A.; Belshaw, L.; Camillis, S. D.; Anumula, S.; Frassetto, F.; Poletto, L.; Palacios, A.; Decleva, P.; Greenwood, J. B.; Martín, F.; Nisoli, M. Ultrafast electron dynamics in phenylalanine initiated by attosecond pulses. *Science* **2014**, *346*, 336−339.
(9) Merritt, I. C. D.; Jacquemin, D.; Vacher, M. Attochemistry: Is controlling electrons the future of photochemistry? *J. Phys. Chem. Lett.* **2021**, *12*, 8404−8415.
(10) Cederbaum, L.; Zobeley, J. Ultrafast charge migration by electron correlation. *Chem. Phys. Lett.* **1999**, *307*, 205−210.
(11) Remacle, F.; Levine, R.; Ratner, M. Charge directed reactivity: a simple electronic model, exhibiting site selectivity, for the dissociation of ions. *Chem. Phys. Lett.* **1998**, *285*, 25−33.
(12) Weinkauf, R.; Schlag, E.; Martinez, T.; Levine, R. Nonstationary electronic states and site-selective reactivity. *J. Phys. Chem. A* **1997**, *101*, 7702−7710.
(13) Ebbesen, T. W. Hybrid light-matter states in a molecular and material science perspective. *Acc. Chem. Res.* **2016**, *49*, 2403−2412.
(14) Herrera, F.; Owrutsky, J. Molecular polaritons for controlling chemistry with quantum optics. *J. Chem. Phys.* **2020**, *152*, No. 100902.
(15) Sidler, D.; Schäfer, C.; Ruggenthaler, M.; Rubio, A. Polaritonic chemistry: Collective strong coupling implies strong local modification of chemical properties. *J. Phys. Chem. Lett.* **2021**, *12*, 508−516.
(16) Xiong, W. Molecular Vibrational Polariton Dynamics: What Can Polaritons Do? *Acc. Chem. Res.* **2023**, *56*, 4845−4850.
(17) Takahashi, S.; Watanabe, K. Decoupling from a thermal bath via molecular polariton formation. *J. Phys. Chem. Lett.* **2020**, *11*, 1349−1356.
(18) Coles, D. M.; Somaschi, N.; Michetti, P.; Clark, C.; Lagoudakis, P. G.; Savvidis, P. G.; Lidzey, D. G. Polariton-mediated energy transfer between organic dyes in a strongly coupled optical microcavity. *Nat. Mater.* **2014**, *13*, 712−719.
(19) Mewes, L.; Wang, M.; Ingle, R. A.; Börjesson, K.; Chergui, M. Energy relaxation pathways between light-matter states revealed by coherent two-dimensional spectroscopy. *Commun. Phys.* **2020**, *3*, 157.
(20) Thomas, A.; Lethuillier-Karl, L.; Nagarajan, K.; Vergauwe, R. M.; George, J.; Chervy, T.; Shalabney, A.; Devaux, E.; Genet, C.; Moran, J.; Ebbesen, T. W. Tilting a ground-state reactivity landscape by vibrational strong coupling. *Science* **2019**, *363*, 615−619.
(21) Hutchison, J. A.; Schwartz, T.; Genet, C.; Devaux, E.; Ebbesen, T. W. Modifying chemical landscapes by coupling to vacuum fields. *Angew. Chem., Int. Ed.* **2012**, *51*, 1592−1596.
(22) Xiang, B.; Ribeiro, R. F.; Dunkelberger, A. D.; Wang, J.; Li, Y.; Simpkins, B. S.; Owrutsky, J. C.; Yuen-Zhou, J.; Xiong, W. Two-dimensional infrared spectroscopy of vibrational polaritons. *Proc. Natl. Acad. Sci. U.S.A.* **2018**, *115*, 4845−4850.
(23) Polak, D.; Jayaprakash, R.; Lyons, T. P.; Martínez-Martínez, L. Á.; Leventis, A.; Fallon, K. J.; Coulthard, H.; Bossanyi, D. G.; Georgiou, K.; Petty, A. J.; et al. Manipulating molecules with strong coupling: harvesting triplet excitons in organic exciton microcavities. *Chem. Sci.* **2020**, *11*, 343−354.
(24) Eizner, E.; Martínez-Martínez, L. A.; Yuen-Zhou, J.; Kéna-Cohen, S. Inverting singlet and triplet excited states using strong light-matter coupling. *Sci. Adv.* **2019**, *5*, No. eaax4482.
(25) Xiang, B.; Ribeiro, R. F.; Du, M.; Chen, L.; Yang, Z.; Wang, J.; Yuen-Zhou, J.; Xiong, W. Intermolecular vibrational energy transfer enabled by microcavity strong light-matter coupling. *Science* **2020**, *368*, 665−667.
(26) Chen, T.-T.; Du, M.; Yang, Z.; Yuen-Zhou, J.; Xiong, W. Cavity-enabled enhancement of ultrafast intramolecular vibrational redistribution over pseudorotation. *Science* **2022**, *378*, 790−794.
(27) Gu, B.; Nenov, A.; Segatta, F.; Garavelli, M.; Mukamel, S. Manipulating core excitations in molecules by x-ray cavities. *Phys. Rev. Lett.* **2021**, *126*, No. 053201.
(28) Cho, D.; Gu, B.; Mukamel, S. Optical Cavity Manipulation and Nonlinear UV Molecular Spectroscopy of Conical Intersections in Pyrazine. *J. Am. Chem. Soc.* **2022**, *144*, 7758−7767.
(29) Gu, B.; Cavaletto, S. M.; Nascimento, D. R.; Khalil, M.; Govind, N.; Mukamel, S. Manipulating valence and core electronic excitations of a transition-metal complex using UV/Vis and X-ray cavities. *Chem. Sci.* **2021**, *12*, 8088−8095.
(30) Sun, S.; Gu, B.; Mukamel, S. Polariton ring currents and circular dichroism of Mg-porphyrin in a chiral cavity. *Chem. Sci.* **2022**, *13*, 1037−1048.
(31) Breidbach, J.; Cederbaum, L. Migration of holes: Formalism, mechanisms, and illustrative applications. *J. Chem. Phys.* **2003**, *118*, 3983−3996.
(32) Remacle, F.; Levine, R. D. Probing ultrafast purely electronic charge migration in small peptides. *Z. Phys. Chem.* **2007**, *221*, 647−661.
(33) Lünnemann, S.; Kuleff, A. I.; Cederbaum, L. S. Ultrafast charge migration in 2-phenylethyl-N, N-dimethylamine. *Chem. Phys. Lett.* **2008**, *450*, 232−235.
(34) Sun, S.; Mignolet, B.; Fan, L.; Li, W.; Levine, R. D.; Remacle, F. Nuclear motion driven ultrafast photodissociative charge transfer of the penna cation: An experimental and computational study. *J. Phys. Chem. A* **2017**, *121*, 1442−1447.
(35) Kuleff, A. I.; Lünnemann, S.; Cederbaum, L. S. Electron-correlation-driven charge migration in oligopeptides. *Chem. Phys.* **2013**, *414*, 100−105.
(36) Vacher, M.; Bearpark, M. J.; Robb, M. A. Communication: Oscillating charge migration between lone pairs persists without significant interaction with nuclear motion in the glycine and Gly-Gly-NH-CH3 radical cations. *J. Chem. Phys.* **2014**, *140*, No. 201102.
(37) Bruner, A.; Hernandez, S.; Mauger, F.; Abanador, P. M.; LaMaster, D. J.; Gaarde, M. B.; Schafer, K. J.; Lopata, K. Attosecond charge migration with TDDFT: Accurate dynamics from a well-defined initial state. *J. Phys. Chem. Lett.* **2017**, *8*, 3991−3996.
(38) Kuleff, A. I.; Cederbaum, L. S. Ultrafast correlation-driven electron dynamics. *J. Phys. B* **2014**, *47*, No. 124002.
(39) Lara-Astiaso, M.; Palacios, A.; Decleva, P.; Tavernelli, I.; Martín, F. Role of electron-nuclear coupled dynamics on charge migration induced by attosecond pulses in glycine. *Chem. Phys. Lett.* **2017**, *683*, 357−364.
(40) Despré, V.; Golubev, N. V.; Kuleff, A. I. Charge migration in propiolic acid: A full quantum dynamical study. *Phys. Rev. Lett.* **2018**, *121*, No. 203002.
(41) Dey, D.; Kuleff, A. I.; Worth, G. A. Quantum Interference Paves the Way for Long-Lived Electronic Coherences. *Phys. Rev. Lett.* **2022**, *129*, No. 173203.
(42) Yong, H.; Sun, S.; Gu, B.; Mukamel, S. Attosecond charge migration in molecules imaged by combined x-ray and electron diffraction. *J. Am. Chem. Soc.* **2022**, *144*, 20710−20716.
(43) Yong, H.; Cavaletto, S. M.; Mukamel, S. Ultrafast valence-electron dynamics in oxazole monitored by x-ray diffraction following a stimulated x-ray raman excitation. *J. Phys. Chem. Lett.* **2021**, *12*, 9800−9806.
(44) Folorunso, A. S.; Bruner, A.; Mauger, F.; Hamer, K. A.; Hernandez, S.; Jones, R. R.; DiMauro, L. F.; Gaarde, M. B.; Schafer, K. J.; Lopata, K. Molecular modes of attosecond charge migration. *Phys. Rev. Lett.* **2021**, *126*, No. 133002.
(45) Mauger, F.; Folorunso, A. S.; Hamer, K. A.; Chandre, C.; Gaarde, M. B.; Lopata, K.; Schafer, K. J. Charge migration and

https://doi.org/10.1021/jacs.3c03821
J. Am. Chem. Soc. 2023, 145, 14856−14864

attosecond solitons in conjugated organic molecules. *Phys. Rev. Res.* **2022**, *4*, No. 013073.
(46) Gu, B.; Mukamel, S. Manipulating nonadiabatic conical intersection dynamics by optical cavities. *Chem. Sci.* **2020**, *11*, 1290−1298.
(47) Gu, B.; Mukamel, S. Optical-cavity manipulation of conical intersections and singlet fission in pentacene dimers. *J. Phys. Chem. Lett.* **2021**, *12*, 2052−2056.
(48) Vendrell, O. Coherent dynamics in cavity femtochemistry: Application of the multi-configuration time-dependent Hartree method. *Chem. Phys.* **2018**, *509*, 55−65.
(49) Vendrell, O. Collective Jahn-Teller interactions through light-matter coupling in a cavity. *Phys. Rev. Lett.* **2018**, *121*, No. 253001.
(50) Mandal, A.; Huo, P. Investigating new reactivities enabled by polariton photochemistry. *J. Phys. Chem. Lett.* **2019**, *10*, 5519−5529.
(51) Schwartz, T.; Hutchison, J. A.; Léonard, J.; Genet, C.; Haacke, S.; Ebbesen, T. W. Polariton dynamics under strong light-molecule coupling. *ChemPhysChem* **2013**, *14*, 125−131.
(52) Suzuki, M.; Nishiyama, K.; Kani, N.; Funahashi, M.; Nakanishi, S.; Tsurumachi, N. Dual-colour pump-probe spectroscopy to observe the transition between polariton branches in an ultrastrongly coupled microcavity containing organic dye molecules. *Jpn. J. Appl. Phys.* **2019**, *59*, No. SCCA08.
(53) Gu, B.; Mukamel, S. Cooperative conical intersection dynamics of two pyrazine molecules in an optical cavity. *J. Phys. Chem. Lett.* **2020**, *11*, 5555−5562.
(54) Galego, J.; Garcia-Vidal, F. J.; Feist, J. Many-molecule reaction triggered by a single photon in polaritonic chemistry. *Phys. Rev. Lett.* **2017**, *119*, No. 136001.
(55) Cavaletto, S. M.; Keefer, D.; Mukamel, S. Electronic coherences in nonadiabatic molecular photophysics revealed by time-resolved photoelectron spectroscopy. *Proc. Natl. Acad. Sci. U.S.A.* **2022**, *119*, No. e2121383119.
(56) Arnold, C.; Larivière-Loiselle, C.; Khalili, K.; Inhester, L.; Welsch, R.; Santra, R. Molecular electronic decoherence following attosecond photoionisation. *J. Phys. B* **2020**, *53*, No. 164006.
(57) Tran, T.; Worth, G. A.; Robb, M. A. Control of nuclear dynamics in the benzene cation by electronic wavepacket composition. *Commun. Chem.* **2021**, *4*, 48.
(58) Gu, B.; Sun, S.; Chen, F.; Mukamel, S. Photoelectron spectroscopy with entangled photons; enhanced spectrotemporal resolution. *Proc. Natl. Acad. Sci. U.S.A.* **2023**, *120*, No. e2300541120.
(59) Dicke, R. H. Coherence in spontaneous radiation processes. *Phys. Rev.* **1954**, *93*, 99.
(60) Tavis, M.; Cummings, F. W. Exact solution for an N-moleculeradiation-field Hamiltonian. *Phys. Rev.* **1968**, *170*, 379.
(61) Wright, A. D.; Nelson, J. C.; Weichman, M. L. Rovibrational Polaritons in Gas-Phase Methane. *J. Am. Chem. Soc.* **2023**, *145*, 5982−5987.
(62) Klimov, A. B.; Chumakov, S. M. *A Group-Theoretical Approach to Quantum Optics: Models of Atom-Field Interactions*; John Wiley & Sons, 2009; pp 113−141.
(63) Campos-Gonzalez-Angulo, J. A.; Ribeiro, R. F.; Yuen-Zhou, J. Generalization of the Tavis-Cummings model for multi-level anharmonic systems. *New J. Phys.* **2021**, *23*, No. 063081.
(64) Campos-Gonzalez-Angulo, J. A.; Yuen-Zhou, J. Generalization of the Tavis-Cummings model for multi-level anharmonic systems: Insights on the second excitation manifold. *J. Chem. Phys.* **2022**, *156*, No. 194308.
(65) Chikkaraddy, R.; De Nijs, B.; Benz, F.; Barrow, S. J.; Scherman, O. A.; Rosta, E.; Demetriadou, A.; Fox, P.; Hess, O.; Baumberg, J. J. Single-molecule strong coupling at room temperature in plasmonic nanocavities. *Nature* **2016**, *535*, 127−130.
(66) Matselyukh, D. T.; Despré, V.; Golubev, N. V.; Kuleff, A. I.; Wörner, H. J. Decoherence and revival in attosecond charge migration driven by non-adiabatic dynamics. *Nat. Phys.* **2022**, *18*, 1206−1213.
(67) He, L.; Sun, S.; Lan, P.; He, Y.; Wang, B.; Wang, P.; Zhu, X.; Li, L.; Cao, W.; Lu, P.; Lin, C. D. Filming movies of attosecond charge migration in single molecules with high harmonic spectroscopy. *Nat. Commun.* **2022**, *13*, No. 4595.
(68) Yu, W.-D.; Liang, H.; Geng, L.; Peng, L.-Y. Dynamical analysis of attosecond molecular modes. *Phys. Rev. A* **2023**, *107*, No. 013101.

https://doi.org/10.1021/jacs.3c03821
J. Am. Chem. Soc. 2023, 145, 14856−14864